

### **Aerosol Science and Technology**



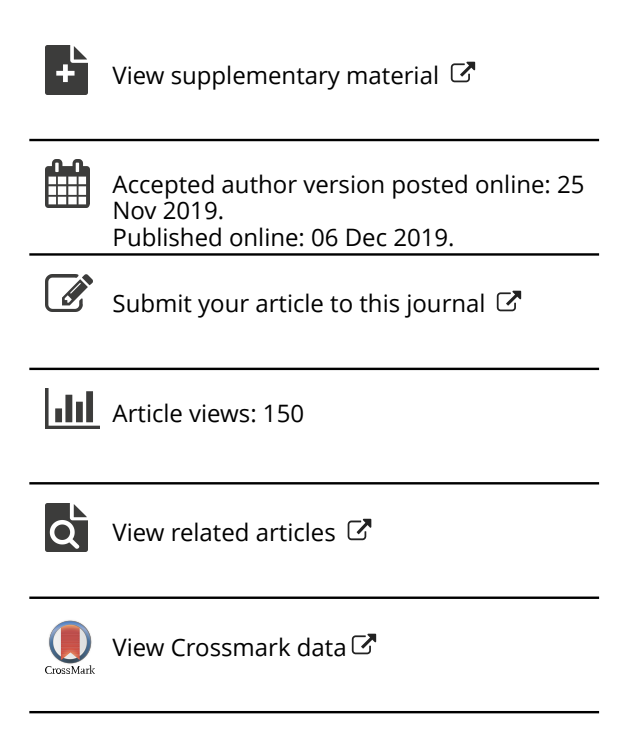
ISSN: 0278-6826 (Print) 1521-7388 (Online) Journal homepage: https://www.tandfonline.com/loi/uast20

# A semi-automated multi-endpoint reactive oxygen species activity analyzer (SAMERA) for measuring the oxidative potential of ambient PM<sub>2.5</sub> aqueous extracts

Haoran Yu, Joseph V. Puthussery & Vishal Verma

**To cite this article:** Haoran Yu, Joseph V. Puthussery & Vishal Verma (2020) A semi-automated multi-endpoint reactive oxygen species activity analyzer (SAMERA) for measuring the oxidative potential of ambient PM<sub>2.5</sub> aqueous extracts, Aerosol Science and Technology, 54:3, 304-320, DOI: 10.1080/02786826.2019.1693492

To link to this article: <a href="https://doi.org/10.1080/02786826.2019.1693492">https://doi.org/10.1080/02786826.2019.1693492</a>









## A semi-automated multi-endpoint reactive oxygen species activity analyzer (SAMERA) for measuring the oxidative potential of ambient PM<sub>2.5</sub> aqueous extracts

Haoran Yu , Joseph V. Puthussery, and Vishal Verma

Department of Civil and Environmental Engineering, University of Illinois at Urbana-Champaign, Urbana, Illinois, USA

#### **ABSTRACT**

Many acellular assays have been developed for assessing the oxidative potential (OP) of ambient PM<sub>2.5</sub>, yet no consensus has been reached on the most appropriate method. Most of these methods are highly time- and labor-intensive, making it difficult to analyze a large sample-set. Here, we have developed a semi-automated multi-endpoint ROS-activity analyzer (SAMERA) for measuring the five most commonly used endpoints of OP: consumption rate of dithiothreitol (OP<sup>DTT</sup>), ascorbic acid (OP<sup>AA-SLF</sup>) and glutathione (OP<sup>GSH-SLF</sup>), and the generation rate of •OH in DTT (OP<sup>OH-DTT</sup>) and in surrogate lung fluid (OP<sup>OH-SLF</sup>). A high analytical precision (coefficient of variation = 5-8% for all endpoints using positive controls such as Cu(II), Fe(II), phenanthrenequinone (PQ) and 5-hydroxy-1,4-naphthoquinone (5-H-1,4-NQ), and 8-13% using PM<sub>2.5</sub> samples) was obtained for SAMERA. The results generated from SAMERA were in good agreement with those obtained from the manual operation using both positive controls (slope = 0.95–1.15 for automated vs. manual,  $R^2 = 0.99$ ) and ambient samples (slope = 0.89–1.09,  $R^2 = 0.86$ –0.97). SAMERA takes 3 h to analyze one sample for all these OP endpoints, which is a substantial improvement over the manual analysis protocol. SAMERA was employed to analyze a subset (N = 44) of ambient PM<sub>2.5</sub> samples collected from the Midwest US. Elevated OP activities in the week of Independence Day (3-5 July, 2018) were observed for most endpoints measured by SAMERA at all the sites. Preliminary results demonstrate the stability and capability of SAMERA for providing a comprehensive OP dataset, which can be integrated into the epidemiological models in future studies.

#### **ARTICLE HISTORY**

Received 13 August 2019 Accepted 6 November 2019

#### **EDITOR**

Jing Wang

#### 1. Introduction

Numerous studies have investigated the adverse health effects of atmospheric particulate matter (PM) to humans (Cohen et al. 2017; Kampa and Castanas 2008; West et al. 2016). The generation of reactive oxygen species (ROS) by fine particles (PM2.5, particles size less than 2.5 µm) has emerged as one of the most promising hypotheses to explain these health effects (Abrams et al. 2017; Bates et al. 2015; Delfino et al. 2013; Maikawa et al. 2016; Sarnat et al. 2016; Yang et al. 2016; Zhang et al. 2016). Many transition metals and organic species present in ambient particles can catalyze the redox reactions in cellular environment, leading to the production of ROS like superoxide radicals ( $\bullet$ O<sub>2</sub><sup>-</sup>), hydroxyl radicals ( $\bullet$ OH) and hydrogen peroxide (H<sub>2</sub>O<sub>2</sub>) (Feng et al. 2016; Longhin et al. 2013; Torres-Ramos et al. 2011). These

species have very high reactivity; for example, the half-lives of •OH and H<sub>2</sub>O<sub>2</sub> are only 10<sup>-9</sup> and 10<sup>-3</sup> s, respectively, in the cellular environment (D'Autréaux and Toledano 2007). •OH can quickly oxidize deoxyribonucleic acid (DNA), proteins and cytoplasmic membrane (Pham-Huy et al. 2008), while H<sub>2</sub>O<sub>2</sub> can target the thiol (-SH) groups in functional proteins such as the enzyme glyceraldehyde-3-phosphate dehydrogenase, and degrades their enzymatic activity (Bonomini et al. 2008). Some of these ROS can be neutralized by the cellular antioxidant defense mechanism (Rahman et al. 2012). The capability of PM to generate ROS and/or consume antioxidants is referred to as the oxidative potential (OP). The OP of ambient PM<sub>2.5</sub> has been linked with multiple health disorders, e.g., atherosclerosis (Araujo and Nel 2009; Sun et al. 2005), asthma (Delfino et al. 2013; Li et al. 2008;

CONTACT Vishal Verma vverma@illinois.edu Department of Civil and Environmental Engineering, University of Illinois at Urbana-Champaign, 205 N. Mathews Ave., Urbana, IL 61801, USA

Color versions of one or more of the figures in the article can be found online at www.tandfonline.com/uast.

■ Supplemental data for this article can be accessed on the publisher's website.

Yang et al. 2016), lung cancer (Knaapen et al. 2004; Oh et al. 2011), and cardiovascular diseases (Chuang et al. 2007; Kodavanti et al. 2000; Weichenthal et al. 2016). These findings indicate that the OP of  $PM_{2.5}$ might be a more relevant indicator in assessing the health outcomes of PM<sub>2.5</sub> compared to their mass concentrations.

To assess the OP of PM, biological assays are considered more representative as they measure the specific biomarkers like interleukin-8 (IL-8) (Becker et al. 2005; Yan et al. 2016) and hemeoxygenase-1 (HO-1) expressions (Crobeddu et al. 2017; Li et al. 2008). However, the time- and labor-intensive experimental protocols of these studies limit their application to only small sample sizes. To overcome these problems, numerous non-biological (i.e., chemical) assays have been developed as substitutes to measure the OP of PM. These chemical assays have the advantages of higher reproducibility, higher accuracy, material cost, and much lesser time and labor.

Among all chemical assays, dithiothreitol (DTT) is the most commonly used probe for measuring the OP of PM (Charrier and Anastasio 2012; Cho et al. 2005; Fang et al. 2014; Verma et al. 2015a). The depletion process of DTT resembles the oxidation of dihydronicotinamide adenine dinucleotide phosphate (NADPH) in mitochondria and the formation of ROS such as •O<sub>2</sub> and H<sub>2</sub>O<sub>2</sub> (Alfadda and Sallam 2012). The consumption rate of DTT (OPDTT) is correlated with the largest pool of PM components, including elemental carbon (EC) (Antiñolo et al. 2015; Saffari et al. 2014), water soluble organic carbon (WSOC) (Verma et al. 2009; Verma et al. 2012), quinones (Charrier and Anastasio 2012), humic-like substances (HULIS) (Verma et al. 2015b), and transition metals (Charrier and Anastasio 2012; Sauvain et al. 2015). OPDTT has also been found to correlate with several biological endpoints, e.g., HO-1 expression (Li et al. 2003), fractional exhaled nitric oxide (Delfino et al. 2013; Zhang et al. 2016), an increased risk of asthma (Yang et al. 2016) and wheeze (Bates et al. 2015). However, ●OH generated through Fenton reaction by Cu(II) or Fe(II) is not represented by DTT depletion rate (Held et al. 1996). In our previous study, Xiong et al. (2017) found that the consumption rate of DTT is well correlated with H<sub>2</sub>O<sub>2</sub> generation, but not with ●OH generation rate in DTT. Therefore, measuring both OPDTT and •OH generation in DTT assay (OPOH-DTT) can provide a wider scope of OP induced by different PM components.

Other than the DTT assay, the consumption rates of several antioxidants present in epithelial lining fluid

have also been used as the indicators of OP. The most commonly indices in this category are the depletion rate of ascorbic acid (AA; OPAA) (Fang et al. 2016; Janssen et al. 2014; Visentin et al. 2016) and reduced glutathione (GSH; OPGSH) (Ayres et al. 2008; Künzli et al. 2006; Mudway et al. 2005). Both OPAA and OPGSH are found to be sensitive to certain transition metals like Fe(II) and Cu(II) (Ayres et al. 2008; Godri et al. 2011; Künzli et al. 2006). A large-scale OP study in the Southeast US found that OPAA has a narrower sensitivity spectrum for PM components and therefore has lesser biological relevance compared to OPDTT (Fang et al. 2016).

A surrogate lung fluid (SLF) containing multiple antioxidants (AA, GSH, uric acid; UA, and citric acid; CA) is generally used to simulate the epithelial lung lining fluid (Charrier et al. 2014), and generation rates of ROS (e.g.,  $\bullet$ OH and  $H_2O_2$ ) in SLF catalyzed by the ambient PM are also used as the indices for OP determination (Charrier and Anastasio 2015; Charrier et al. 2014; Shen et al. 2011). Previous studies have shown that Cu(II) dominated the generation of H<sub>2</sub>O<sub>2</sub> in SLF (96%) (Charrier et al. 2014), while both Cu(II) and Fe(II) contributed to •OH generation (up to 92%) in SLF (OPOH-SLF) (Charrier and Anastasio 2015). Quinone compounds contributed marginally (at most 4% and 8% for  $H_2O_2$  and  $\bullet OH$ , respectively) to the generation of ROS in SLF.

Although various chemical assays have been developed to quantify the OP of ambient PM, no consensus has been reached in the scientific community for selecting the most appropriate method. Among several available OP endpoints, OP<sup>DTT</sup>, OP<sup>OH-DTT</sup>, OP<sup>AA</sup>,  $\mathsf{OP}^\mathsf{GSH}$  and  $\mathsf{OP}^\mathsf{OH}\text{-}\mathsf{\widehat{SLF}}$  are the ones, which have shown some promises in terms of their biological relevance (Abrams et al. 2017; Bates et al. 2015; Janssen et al. 2015; Ma et al. 2015; Maikawa et al. 2016; Wang et al. 2018; Weichenthal et al. 2016; Yang et al. 2016). These five endpoints are highly reproducible and cover the ROS-expression pathways by most of the redox active PM components. However, each of these methods takes 1-2h to perform, thus consuming almost one graduate student - day to analyze one sample. To overcome this limitation, we have developed an automated instrument, which measures all these OP endpoints for a given ambient PM aqueous The instrument named Semiextract in 3 h. Automated Multi-Endpoint ROS-activity Analyzer (SAMERA) is developed from the prototype of a semi-automated DTT activity system described in Fang et al. (2014), and is able to serve for 24-h unattended sample analysis. We tested the response of SAMERA using select sensitive chemical compounds for individual endpoints. We also evaluated the performance of SAMERA for both precision and accuracy using positive controls and water-soluble ambient PM<sub>2.5</sub> extracts. The OP results of ambient samples on all the endpoints are compared with those reported in previously published studies. Finally, we demonstrated the potential application of SAMERA by analyzing a subset of large number of ambient PM<sub>2.5</sub> samples collected from the Midwest US.

#### 2. Materials and methods

#### 2.1. Chemicals

AA, CA, UA, GSH, DTT, 9,10-Phenanthrenequinone (PQ), 5-hydroxy-1,4-naphthoquinone (5-H-1,4-NQ), 2-hydroxyterephthalic acid (2-OHTA), 5,5'-dithiobis-(2-nitrobenzoic acid) (DTNB), o-phthaldialdehyde sulfate (OPA), copper (II)pentahydrate sulfate heptahydrate  $(CuSO_4 \bullet 5H_2O),$ iron (II)potassium phosphate  $(FeSO_4 \bullet 7H_2O),$ monobasic (KH<sub>2</sub>PO<sub>4</sub>) and potassium phosphate dibasic (K<sub>2</sub>HPO<sub>4</sub>) were obtained from Sigma-Aldrich (St. Louis, MO, USA). Sodium hydroxide (NaOH) was obtained from VWR International Inc. (Radnor, PA, USA). Disodium terephthalate (TPT) was obtained from Alfa Aesar (Tewksbury, MA, USA).

The stock solutions of 20 mM AA, 30 mM CA, 10 mM UA and 10 mM GSH were made in 10 mL deionized water (DI; Milli-Q; resistivity = 18.2 M $\Omega$ /cm) separately, stored at 4°C in the refrigerator, and used within one week. 50 µL of 4 M NaOH was added into UA stock solution to adjust pH and dissolve UA. SLF solution was made fresh daily by mixing equal volumes (1 mL each) of four antioxidant stock solutions and diluting the mixture by DI to 10 mL. The stock solution of 10 mM DTT was made and stored in the refrigerator for at most two months. DTT solution used in SAMERA was made daily by diluting 1 mL of DTT stock solution into 10 mL DI. 0.5 mM potassium phosphate buffer (K-PB; pH = 7.4) was prepared by dissolving 26.94 g KH<sub>2</sub>PO<sub>4</sub> and 139.70 g K<sub>2</sub>HPO<sub>4</sub> in 2 L of DI. 50 mM TPT solution was made by dissolving 5.31 g TPT in 500 mL of 0.5 mM K-PB. 10 mM DTNB stock solution was prepared in methanol and stored in the refrigerator for no longer than two months. 0.2 mM DTNB solution used in SAMERA was made weekly by diluting 10 mL of DTNB stock solution into 500 mL of DI. 2 mM OPA solution was made by dissolving 134.1 mg of OPA in 1 mL methanol, followed by dilution with DI to 500 mL. 10 mM PQ and 5-H-1,4-NQ stock solutions were made in

DMSO every day prior to the experiments. The stock solutions of 10 mM CuSO<sub>4</sub> and 10 mM FeSO<sub>4</sub> were prepared in DI every day prior to the experiments. The final solutions for the positive control chemicals (i.e., PQ, 5-H-1,4-NQ, Cu(II) and Fe(II)) were obtained by serially diluting the stock solutions in DI.

#### 2.2. System setup

The schematic diagram of SAMERA is shown in Figure 1a. SAMERA consists of three major parts: sample injection, sample incubation, and measurement system. The sample injection system includes three Kloehn programable syringe pumps (IMI precision, Littleton, CO, USA) and a 14-port multi-position valve (VICI® Valco Instrument Co. Inc., Houston, TX, USA). The Kloehn syringe pumps serve for dispensing the solutions between chemical reservoirs, various vials and the flow cells. The multi-position valve connects the sample vials to one of the syringe pumps (Pump 2) and is controlled by a valve actuator (VICI<sup>®</sup>), which consecutively selects different samples for analysis. The sample incubation Eppendorf employs an ThermoMixer system (Eppendorf North America, Hauppauge, NY, USA) for holding and incubating three centrifuge tubes (also called reaction vials, RV1, RV2 and RV3) at a constant temperature (37 °C), while continuously shaking at a frequency of 400 rpm. There are two components in the measurement system – a spectrophotometer and a spectrofluorometer. The spectrophotometer (Ocean Optics, Dunedin, FL, USA) consists of an ultraviolet-visiblenear-infrared (UV - Vis-NIR) light source as well as a multiwavelength light detector, and is used for detecting the absorbance of the targeted compound in OPAA and OP<sup>DTT</sup> analyses. The Fluoromax-4 spectrofluorometer (Horiba Scientific, Edison, NJ, USA) serves to measure the fluorescence of the indicator compounds for the determination of GSH and •OH.

#### 2.3. OP analysis protocol

The algorithm for OP analysis in SAMERA is shown in Figure 1b. The five endpoints are measured in two separate stages. OP<sup>AA-SLF</sup>, OP<sup>GSH-SLF</sup> and OP<sup>OH-SLF</sup> are measured in the first stage following an SLF-based protocol, while a DTT assay is conducted to measure OP<sup>DTT</sup> and OP<sup>OH-DTT</sup> in the second stage. Since the consumption of AA and GSH was measured in SLF in our study, we have denoted these OP endpoints as OP<sup>AA-SLF</sup> and OP<sup>GSH-SLF</sup>, to distinguish them from the studies directly measuring AA and GSH without any SLF (simply denoted as OP<sup>AA</sup> and OP<sup>GSH</sup> here).

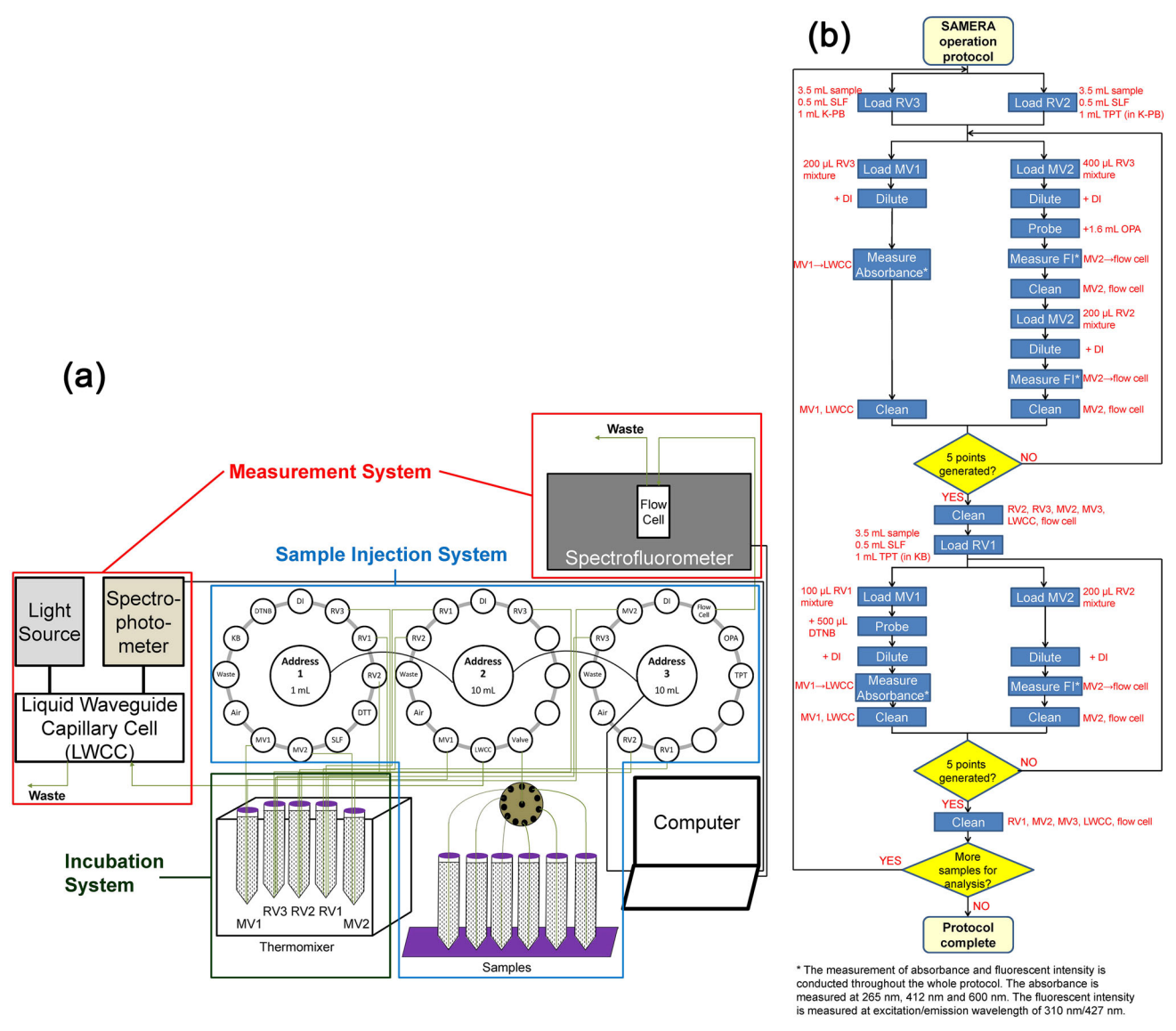


Figure 1. The system setup (a) and algorithm (b) of Semi-Automated Multi-Endpoint ROS Activity Analyzer (SAMERA).

#### 2.3.1. SLF-based protocol

The SLF-based protocol involves three steps. In the first (incubation) step, 3.5 mL of the sample (either PM filter extract or chemical standard), 1 mL of K-PB (pH = 7.4) and 0.5 mL of SLF (final concentrations of AA, GSH, UA and CA in RV as 200 μM, 100 μM, 100 μM, and 300 μM, respectively following Charrier and Anastasio [2015] protocol) are loaded separately into RV2 and RV3 kept in the ThermoMixer through injection system (see Figure 1a). The only difference in the content of RV2 and RV3 is that the K-PB in RV2 contains TPT (50 mM) to immediately capture the •OH generated in the reaction. In the second (probing) step, two small aliquots (200 μL and 400 μL) are withdrawn separately from RV3 using the same injection system, and transferred to the measurement vials 1 and 2 (MV1 and MV2), respectively. This injected mixture is diluted by DI in MV1 for measuring AA, while 1.6 mL of OPA is added into MV2 for probing GSH in the injected mixture. GSH reacts with OPA, forming a fluorescent product (referred as GS-OPA hereafter), which can be detected by a spectrofluorometer (Böhmer et al. 2011). In the third (measurement) step, the diluted mixture in MV1 is withdrawn from the vial and pushed through a liquid waveguide capillary cell (LWCC-3100; Precision Instruments, Inc., Sarasota, FL, USA), where the absorbance at 265 nm and 600 nm (background) is measured by the spectrophotometer and is recorded by Ocean Optics SpectraSuite software. The background corrected absorbance at 265 nm (Abs<sub>265nm</sub> -Abs<sub>600nm</sub>) is used to determine the concentration of residual AA in RV2. Similarly, the mixture in MV2 is further diluted and injected into the flow cell of the

spectrofluorometer. The fluorescence intensity is measured at the excitation/emission wavelength of 310 nm/ 427 nm, to determine the concentration of GS-OPA. Although the peak absorbance and emission of GS-OPA is at 340 nm and 420 nm wavelength (Roušar et al. 2012), an excitation/emission wavelength of 310/ 427 nm with a slit width of 5 nm is selected to allow the measurement of both GS-OPA and 2-OHTA (fluorescent product of •OH and TPT, discussed later), without the need of changing the slit position. Figure S1 in the supplemental information (SI) shows the contour plot of fluorescence intensity and calibration curves at different excitation/emission wavelengths for GS-OPA, indicating no significant difference for GS-OPA measurement at either of these wavelengths settings. The MVs and flow cells are cleaned with DI immediately after each measurement step. Steps 2 and 3 are repeated five times at designated time intervals (i.e., 5 min, 24 min, 43 min, 62 min, and 81 min) to determine the consumption rate of AA and GSH. Calibration curves to quantify AA and GSH are prepared by measuring initial absorbance and fluorescence intensity of different known concentrations of AA and GSH in SLF, following the same protocol as described above. The consumption rate of both AA and GSH is then derived from these calibration curves.

The measurement of •OH is conducted around the same time as GSH and AA. TPT present in RV2 reacts with •OH and forms a fluorescent product: 2-OHTA. At designated time intervals (i.e., 10 min, 29 min, 48 min, 67 min, and 86 min), a small aliquot (200 μL) of the reaction mixture in RV2 is withdrawn into MV2, and diluted by DI. The diluted mixture in MV2 is then passed through the flow cell of the spectrofluorometer. The peak absorbance of 2-OHTA is at 310 nm, while the emission intensity peaks at 427 nm. Therefore, the same wavelength settings (as used for the GS-OPA measurements) are used to determine the concentration of 2-OHTA. The concentration of 2-OHTA in the reaction mixture is derived by calibrating the spectrofluorometer with known concentrations (0-200 nM) of 2-OHTA standards. The concentrations of •OH are then calculated after dividing 2-OHTA concentration by 0.35 - the yield of 2-OHTA from the reaction between TPT and •OH (Son et al. 2015). The flow cell and MV2 are cleaned with DI immediately after the measurement. After completing all the measurements of AA, GSH in RV3 and •OH in RV2 at different time intervals, SAMERA performs a final cleaning of all the vials (i.e., RV2, RV3, MV1 and MV2), connection tubes and flow cells by rinsing them with DI, to prepare the system for the DTT assay.

#### 2.3.2. DTT assay

The protocol of DTT assay is adapted from our previous publication (Yu et al. 2018), and combines the •OH generation measurement into the automated OP<sup>DTT</sup> analysis protocol, following the same three step process as in SLF-based protocol. In the first incubation step, 3.5 mL of sample, 0.5 mL of 1 mM DTT and 1 mL of 50 mM K-PB-buffered TPT are added into RV1. Our tests have shown that the addition of TPT in the reaction vial does not affect the consumption rate of DTT (see Section S2 and Figure S2 in SI). At specific time intervals (5 min, 17 min, 29 min, 41 min, and 53 min), a small aliquot (100 μL) of the reaction mixture from RV1 is taken out and added to 500 µL of 200 µM DTNB in measurement vial 1 (MV1) (probing step). DTNB combines with residual DTT in the mixture, and forms a yellow colored complex, 2-nitro-5-thiobenzoic acid (TNB). The mixture in MV1 is then diluted and passed through LWCC, where the absorbance at 412 nm and 600 nm (background) is measured by the spectrophotometer and recorded by Ocean Optics SpectraSuite software. A DTT calibration curve is also prepared by measuring the initial absorbance of different known concentrations of DTT (0-100 µM). Simultaneously with the DTT measurement (i.e., 5 min, 17 min, 29 min, 41 min, and 53 min), another aliquot (200 μL) of the mixture from RV1 is withdrawn and diluted with DI in MV2. The measurement of •OH then follows in the same manner as •OH concentration in SLF. All MVs and flow cells are cleaned with DI immediately after each measurement step.

After all, five endpoints are measured for a given sample, SAMERA performs a final self-cleaning operation for all RVs, MVs, LWCC and flow cell by rinsing them with DI, before the next run of analysis. The next sample is selected by the multi-position valve using VCOM software. The system is thoroughly cleaned at least three times every week by replacing all the reagents and chemicals with DI and run the same code as for the sample analysis. The procedure for mass and volume normalized OP (OPm and OPv, respectively) determination from the raw absorbance and fluorescence intensity data is described in the SI (Section S3 and Figure S3).

#### 2.4. Ambient samples collection and preparation

#### 2.4.1. Sampling

Ambient  $PM_{2.5}$  samples were collected on prebaked quartz filters (Pall Tissuquartz<sup>TM</sup>, 8" × 10") using high-volume samplers (flow rate =  $1.13 \, \text{m}^3/\text{min}$ ;

PM<sub>2.5</sub> inlets, Tisch Environmental; Cleves, OH) installed at five sites in the Midwest US. The map of all sites is shown in Figure S4 in SI. Champaign (CMP) site is located on a parking garage (~30 m from ground level) in the campus of University of Illinois at Urbana-Champaign (UIUC) and is adjacent to a major road (University Ave.) in Urbana, IL. Bondville (BON) site is located in a rural area, 15 km west of downtown Champaign. Chicago (CHI) site is located on the rooftop (~40 m from the ground level) of a student dormitory building (Carman hall) in Illinois Institute of Technology (IIT) campus, which is 0.5 km east of a 6-lane interstate highway I-90/94 and 1.5 km west of Lake Michigan. Indianapolis (IND) site is located in the campus of Indiana University -Purdue University Indianapolis (IUPUI) and is close to downtown Indianapolis (2 km southeast of the site) and a 4-lane interstate highway I-65 (1 km northeast of the site). St. Louis (STL) site is located in the north-central area of St. Louis (3247 Blair St.), and is part of the National Core Pollutants (NCore) Network of USEPA. The site is surrounded by multiple industries for steel and vehicle part fabrication.

All PM<sub>2.5</sub> samples analyzed in the current study were collected for a sampling duration of 72 h in the months of May, June and July 2018. The samples used for assessing the precision and accuracy of SAMERA (discussed in Section 2.5) were collected separately at CMP site (N = 10). Sufficient field blank filters (N = 10) were also collected during the sampling. The exact dates of filter collection for different experiments are provided in Table S1 (SI). All filter samples were weighed before and after PM<sub>2.5</sub> collection using a lab-scale digital balance (±0.2 mg readability; Sartorius A120S, Götingen, Germany) for determining PM mass loadings on the filters. The filters were equilibrated for at least 24 h in a control room with constant temperature (20°C) and relative humidity (RH = 50%) before weighing. The filters were wrapped in prebaked (at 550 °C) aluminum foils and stored in a freezer at  $-20\,^{\circ}$ C immediately after weighing.

#### 2.4.2. PM extraction from the filters

Before analysis, a few (usually 2-5) punches (1" diameter each) were taken from the PM<sub>2.5</sub> filters by a metallic punch, and extracted in 20 mL DI using an ultrasonic water bath (Cole-Palmer, Vernon-Hills, IL, USA). These extracts were filtered through a 0.45 µm polytetrafluoroethylene (PTFE) syringe filter to remove the insoluble components. The filtered extracts were then analyzed by SAMERA for all five OP endpoints (i.e., OPAA-SLF, OPGSH-SLF, OPOH-SLF, OPDTT and OPOH-DTT).

#### 2.5. Performance evaluation of SAMERA

The performance of SAMERA was evaluated by measuring the limit of detection (LOD), instrument response, precision and accuracy for five OP endpoints using blanks, positive controls and ambient samples. The LOD was obtained by analyzing multiple blanks (both DI and field blank filters). Four redoxactive chemicals (Cu(II), Fe(II), PQ and 5-H-1,4-NQ) were selected as the positive controls to test the instrument response for five endpoints. Precision was assessed by analyzing the same sample multiple times, while accuracy was determined by comparing the results obtained from SAMERA with that from the manual analysis of a given set of samples (discussed in next section). All OP assays on the positive controls for assessing instrument response, precision and accuracy were conducted in triplicates.

#### 3. Results and discussions

#### 3.1. Limit of detection (LOD)

The LOD of SAMERA is defined as three times of the standard deviation of OP activities for blanks. Both DI and field blank filters were used as the blanks for assessing LOD. Table 1 lists the average blank level and LOD for five OP endpoints. The LOD determined from DI is useful to determine the minimum concentration of chemical standards, which are prepared in DI, while that from field blanks is important for the ambient PM samples. However, the expression of LOD in terms of the PM mass is complicated as it depends on many factors, such as extraction protocol (e.g., volume of water used for PM extraction and the filter area which can be submerged in that volume), and the concentration of redox-active substances in the PM. In previous studies, at least 50 µg/mL of PM in the reaction mixture was generally used for OPAA and OPGSH measurements (Ayres et al. 2008; Künzli

Table 1. The average blank levels and LOD of SAMERA for five OP endpoints as measured from both DI blanks and field blank filters.

		DI blank		Filter blan	Filter blank filters	
Endpoint	Unit	Average	LOD	Average	LOD	
OP <sup>AA-SLF</sup> OP <sup>GSH-SLF</sup> OP <sup>OH-SLF</sup> OP <sup>OH-DTT</sup>	μM/min μM/min nM/min μM/min nM/min	0.150 0.297 3.390 0.496 -0.463	0.197 0.144 1.824 0.060 0.634	0.169 0.368 4.570 0.651 -0.385	0.210 0.165 3.633 0.065 0.724	

et al. 2006; Mudway et al. 2005), while  $OP^{DTT}$  was found to be sensitive enough even at  $10\,\mu g/mL$  of PM (Charrier et al. 2016; Fang et al. 2014). Based on the analysis of ten ambient samples at different concentrations in this study, we found that the endpoints  $OP^{DTT}$  and  $OP^{OH-SLF}$  are sufficiently above detection at  $10\,\mu g/mL$ , while other endpoints require higher concentrations –  $30\,\mu g/mL$  for  $OP^{OH-DTT}$  and  $50\,\mu g/mL$  for  $OP^{AA-SLF}$  and  $OP^{GSH-SLF}$ . Therefore, to obtain a good performance of SAMERA for all the endpoints, we recommend using a minimum concentration of  $50\,\mu g/mL$  for SLF-based assays, and  $30\,\mu g/mL$  for DTT-based assays.

#### 3.2. The response of SAMERA to positive controls

Four chemicals – Cu(II), Fe(II), PQ and 5-H-1,4-NQ, were selected as the positive controls separately for five OP endpoints based on their reported sensitivities, i.e., Cu(II) for OPAA-SLF and OPGSH-SLF (Ayres et al. 2008; Mudway et al. 2005), Fe(II) for OPOH-SLF (Charrier and Anastasio 2015; Vidrio et al. 2008), PQ for OPDTT (Cho et al. 2005; Xiong et al. 2017), and 5-H-1,4-NQ for OPOH-DTT (Xiong et al. 2017; Yu et al. 2018). All the calibration curves for different OP endpoints using these positive controls yield an excellent coefficient of determination ( $R^2 = 0.96-0.99$ ), as shown in Figure 2. The slope of the calibration curve for  $OP^{DTT}$  (6.92 ± 0.16 min<sup>-1</sup>) is close to the one obtained by Fang et al. (2014) in the automated system based on the DTT assay  $(7.64 \pm 0.51 \,\mathrm{min}^{-1})$ , adding confidence to the measurements obtained by SAMERA.

#### 3.3. Precision

The analytical precision of SAMERA was assessed by analyzing ten parallel samples, i.e., respective positive controls of same concentration for each OP endpoint. The average and standard deviation of the OP activities measured from these analyses are listed in Table 2. A low coefficient of variation (CoV) for all five OP endpoints (4.9%-8.1%) indicates a high reproducibility of the results obtained from SAMERA.

Overall precision of SAMERA was assessed by using ambient  $PM_{2.5}$  samples for five endpoints. Ten punches – each of 1" diameters were taken from the same Hi-Vol filter collected at CMP site, and extracted separately in 10 mL DI water. After filtering through a 0.45  $\mu$ m PTFE syringe filter, the extracts were analyzed by SAMERA for all five endpoints. Table 3 lists the average and standard deviation of

the mass-normalized OP activities (OPm) for five endpoints. A slightly higher CoV (7.9–13.3%) compared to that by the positive controls is observed, which is reasonable due to higher uncertainties associated with extraction procedures, e.g., non-uniform mass loadings on the filter and variable PM extraction efficiencies.

#### 3.4. Accuracy

SAMERA was validated for accuracy through comparison of its results with that from the manual operation, over a range of concentrations (same as used in Figure 2) of positive controls. Figure 3 shows the comparison of OP measured by manual operation (X axis) with that from SAMERA (Y axis) for all five endpoints using positive controls. The fitted lines from orthogonal regressions applied on two measurement approaches (i.e., automated vs. manual) yield slopes close to 1 (OP<sup>AA-SLF</sup>:  $1.15 \pm 0.07$ ; OP<sup>GSH-SLF</sup>:  $0.95 \pm 0.07$ ; OP<sup>OH-SLF</sup>:  $0.95 \pm 0.05$ ; OP<sup>OH-DTT</sup>:  $0.96 \pm 0.05$ ), with an excellent coefficient of determination (R<sup>2</sup> > 0.98), indicating high accuracy of SAMERA as tested from the positive controls.

Accuracy was also tested using ambient samples. Nine ambient PM<sub>2.5</sub> Hi-Vol filter samples collected at CMP site were extracted and analyzed for all five endpoints using both SAMERA and the manual operation. Figure 4 shows comparison of the mass-normalized OP activities (OPm) measured from two approaches for all five endpoints. Similar to positive controls, the slopes of the regression curves from the orthogonal fit of two measurement methods on five  $(OP^{AA-SLF}:$ OP<sup>GSH-SLF</sup>: endpoints  $0.97 \pm 0.07$ ;  $0.99 \pm 0.09$ ; OP<sup>OH-SLF</sup>:  $0.98 \pm 0.15$ ; OP<sup>DTT</sup>:  $1.09 \pm 0.08$ ;  $OP^{OH\text{-}DTT}\!\!:\,0.89\pm0.14)$  were close to 1, with high  $R^2$ (0.86-0.97). A 2-tailed paired t-test further demonstrates no significant differences (p > 0.05) in the results obtained from two measurement approaches (i.e., manual and automated) using both positive controls and the ambient samples.

#### 3.5. Field application of SAMERA

An important objective of developing SAMERA is to employ it for generating large OP dataset. This dataset could then be integrated into epidemiological studies for testing the hypothesis of OP association with biological health endpoints. Therefore, we tested utility and stability of SAMERA by analyzing a subset of our large number of ambient PM samples (N  $\sim$ 300) collected from five sites in the Midwest US. Note, the

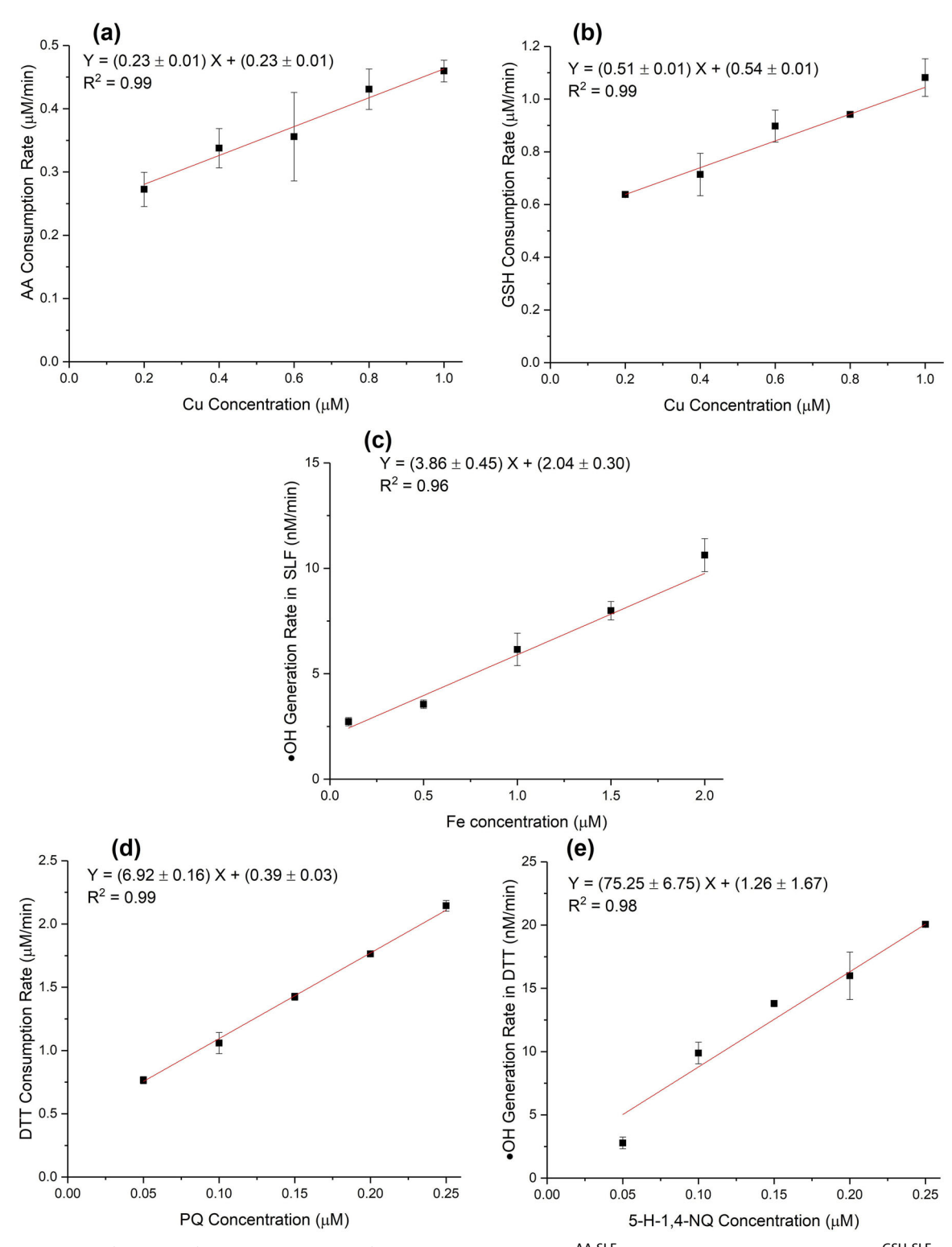


**Figure 2.** OP as a function of the concentration of positive controls: (a) OP<sup>AA-SLF</sup> vs. Cu(II) concentrations; (b) OP<sup>GSH-SLF</sup> vs. Cu(II) concentrations; (c) OP<sup>OH-SLF</sup> vs. Fe(II) concentrations; (d) OP<sup>DTT</sup> vs. PQ concentrations; (e) OP<sup>OH-DTT</sup> vs. 5-H-1,4-NQ concentrations. The error bars represent the standard deviation of triplicate OP analysis.

complete OP analysis along with a comprehensive chemical and toxicity characterization of these samples is currently underway and this will be a topic of our future manuscripts. Here, we show a snapshot of the data from only 44 samples collected during summer 2018, from the perspective of demonstrating the potential application of SAMERA in yielding an important OP dataset. All filters were extracted in DI and therefore only water-soluble fraction was analyzed.

**Table 2.** Precision of SAMERA as obtained by multiple (N = 10) measurements of various standard chemicals.

		Standard		Standard	
Endpoint	Unit	Chemical	Average	Deviation	CoV (%)
OP <sup>AA-SLF</sup>	μM/min	1 μM Cu(II)	0.405	0.033	8.11
OP <sup>GSH-SLF</sup>	μM/min	1 μM Cu(II)	0.737	0.044	6.03
OP <sup>OH-SLF</sup>	nM/min	2 μM Fe(II)	11.74	0.83	7.10
OP <sup>DTT</sup>	μM/min	0.2 μM PQ	1.867	0.094	5.04
OP <sup>OH-DTT</sup>	nM/min	0.2 μM 5-H-1,4-NQ	15.83	0.77	4.89

The concentration of the standard chemical refers to concentration in the reaction vial. CoV is the percentage ratio of the standard deviation to the average level.

**Table 3.** Precision of SAMERA as obtained by multiple (N = 10) measurements of an ambient PM<sub>2.5</sub> sample.

Endpoint	Unit	Average	Standard Deviation	CoV (%)
OP <sup>AA-SLF</sup>	nmol/(min·μg)	0.0166	0.00196	11.87
OP <sup>GSH-SLF</sup>	nmol/(min·μg)	0.0281	0.00221	7.89
OP <sup>OH-SLF</sup>	nmol/(min·μg)	0.437	0.0462	10.56
OP <sup>DTT</sup>	pmol/(min·μg)	0.0367	0.00387	10.52
OP <sup>OH-DTT</sup>	pmol/(min·μg)	0.0489	0.00650	13.28

Figure 5 shows the time series of both mass-normalized and volume-normalized OP endpoints. From the comparison of OPm, a substantial variation could be observed among the sites for several endpoints. For example, the samples from CMP had higher activities for OPAA-SLFm, OPGSH-SLFm and OPOH-SLFm endpoints than other sites. Our previous studies have observed significant concentrations of Cu (5-52 ng/ m<sup>3</sup>) at this site (Puthussery et al. 2018; Wang et al. 2018), which is an important driver of these endpoints. Because CMP is adjacent to a major road (University Ave.), the emissions from brake wear and dust resuspension (Hulskotte et al. 2007) could contribute to Cu at this site. In contrast, CHI had higher activities for OPOH-SLFm, OPDTTm and OPOH-DTTm endpoints compared to IND and STL. In volume normalized activities (Figure 5b), a similar trend but with lesser variation than OPm among these sites can be observed for all five endpoints. Figure S5 in SI shows the ambient concentrations of PM<sub>2.5</sub> mass at all these sites, which seem to have only marginal variations, except STL (higher levels than others). A significant variation in the mass normalized activities despite similar ambient concentration profiles of PM<sub>2.5</sub> mass indicates that the composition of redox-active PM fraction varies substantially among these sites.

The activities for most OP endpoints (OP<sup>AA-SLF</sup>, OP<sup>GSH-SLF</sup>, OP<sup>DTT</sup>, and OP<sup>OH-SLF</sup>) were elevated in the week of July 3 at all sampling sites. This trend is more profound in OPv than in OPm, except at BON (due to lower ambient PM mass concentration there in that week; see Figure S5 in SI). This is attributed to the fireworks emissions for the Independence Day celebration on the evening of July 4. In our previous

study, Puthussery et al. (2018) also observed elevated OP levels of ambient  $PM_{2.5}$  on July 4, 2017 in Urbana, IL using a real-time  $OP^{DTT}$  instrument. Cracking fireworks result into elevated levels of ambient Fe and Cu (Pervez et al. 2016), which are intrinsically ROS-active in most of these assays.

Table 4 shows the comparison of average massnormalized and volume-normalized OP activities measured in this study with several previous studies conducted in North America, Europe, China and India. OP<sup>AA</sup>v (Table 4a) measured in this study  $(0.044-0.745 \,\mathrm{nmol \cdot min^{-1} \cdot m^{-3}})$  is at very low end of the range (0.2-5.2 nmol·min<sup>-1</sup>·m<sup>-3</sup>) reported by Fang et al. (2016) for the ambient PM<sub>2.5</sub> samples collected from Southeast US. However, the range of our OPAA-<sup>SLF</sup>m  $(0.004-0.077 \text{ nmol·min}^{-1} \cdot \mu\text{g}^{-1})$  measurements is closer to the range  $(0.0017-0.04 \,\mathrm{nmol \cdot min}^{-1} \cdot \mu \mathrm{g}^{-1})$ reported by Szigeti et al. (2016) for the urban PM<sub>2.5</sub> samples collected from 20 European cities. The median of our OP<sup>AA-SLF</sup>m (0.012 nmol·min<sup>-1</sup>·µg<sup>-1</sup>) is also close to the average activity reported in two European studies (Künzli et al. 2006; Mudway et al. 2005). Since OPAAv in Fang et al. (2016) was measured in the absence of other antioxidants (i.e., GSH, UA, and CA), the lower OPAA-SLFv in our study might be due to the interactions among these antioxidants. For example, GSH has the ability to reduce the oxidized AA (Birben et al. 2012), thereby slowing down depletion rate of AA in SLF. Recently, Pietrogrande et al. (2019) has also reported a significant suppressing effect by other three antioxidants (i.e., GSH, CA, and UA, up to 80% decrease depending upon the relative concentrations of these antioxidants) in SLF on the consumption rate of AA.

Our OP<sup>GSH-SLF</sup>m (Table 4b) has a slightly wider range  $(0.001-0.040 \text{ nmol}\cdot\text{min}^{-1}\cdot\mu\text{g}^{-1})$  than the range  $(0-0.0275 \text{ nmol·min}^{-1} \cdot \mu \text{g}^{-1})$  reported in the studies conducted so far. Note, the depletion rate of both AA and GSH reported in most studies (Godri et al. 2011; Künzli et al. 2006; Mudway et al. 2005; Szigeti et al. 2016) are calculated based on a 4-h test with the lung lining fluid (200 µM AA, 200 µM GSH and 200 µM UA), which has a different composition than the SLF used in this study (200 µM AA, 100 µM GSH, 100 µM UA and 300 µM CA). Furthermore, a photometricbased DTNB enzymatic recycling assay adapted from Baker et al. (1990) was used for GSH determination in all these studies. In this assay, DTNB reacts with GSH and generates oxidized glutathione (GSSG) and TNB, while GSSG is reduced back to GSH by an additional reductant NADPH, catalyzed by glutathione reductase (GR). TNB production (i.e., absorbance at

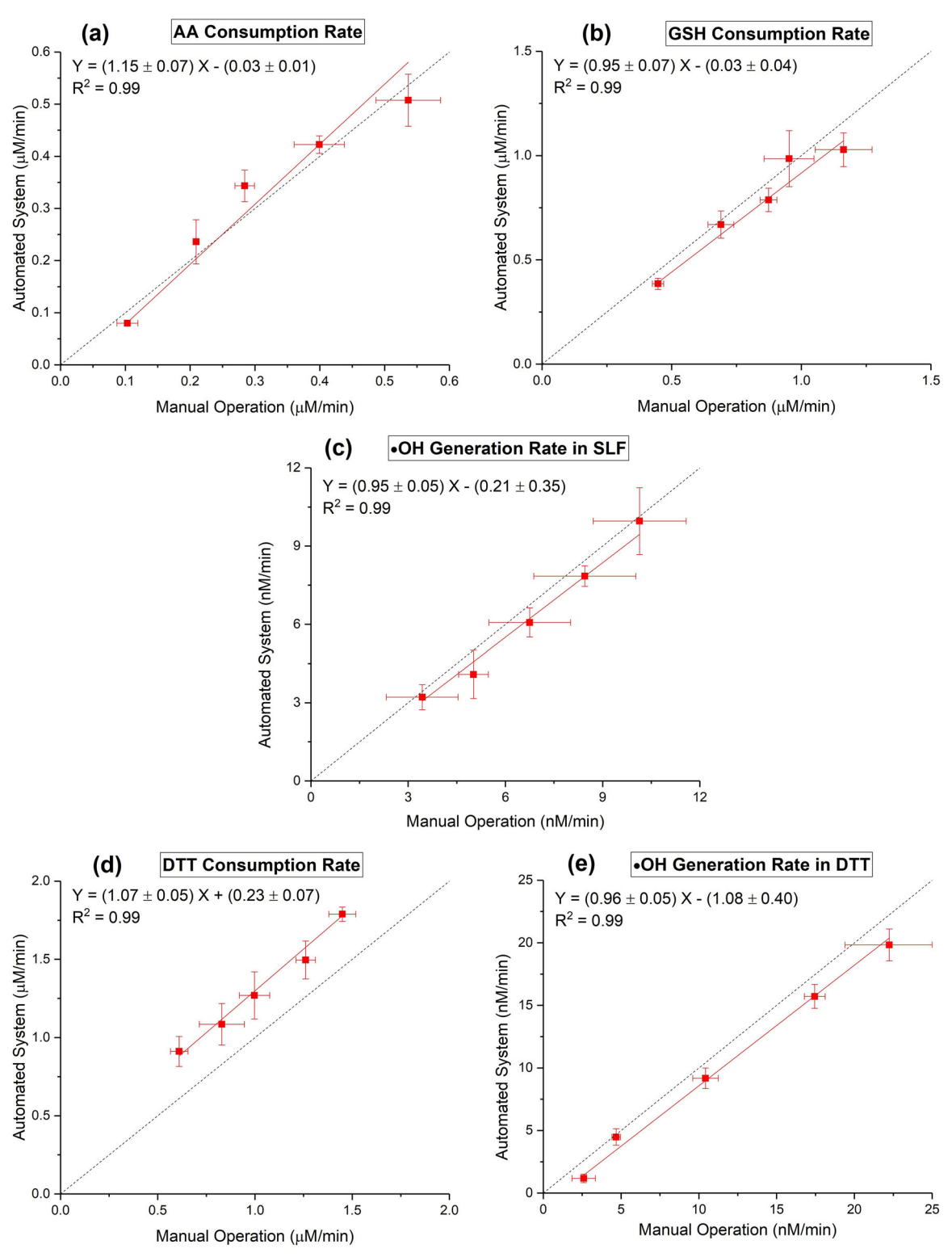


**Figure 3.** Comparison of manual operation (X axis) and automated system (Y axis) using four positive controls: (a) OP<sup>AA-SLF</sup> of Cu(II); (b) OP<sup>GSH-SLF</sup> of Cu(II); (c) OP<sup>OH-SLF</sup> of Fe(II); (d) OP<sup>DTT</sup> of PQ; (e) OP<sup>OH-DTT</sup> of 5-H-1,4-NQ. The error bars on X and Y axes denote the standard deviation of triplicate OP analysis by both manual operation and automated system, respectively. The identity line is plotted as the dotted line.

412 nm) is measured to determine the concentration of total glutathione (GSSG and GSH) and GSSG (by first removing GSH using 2-vinylpyridine). GSH

concentration is then obtained indirectly by subtracting 2 times of GSSG from total GSH (Mudway et al. 2001). This method has been adapted from the cell-

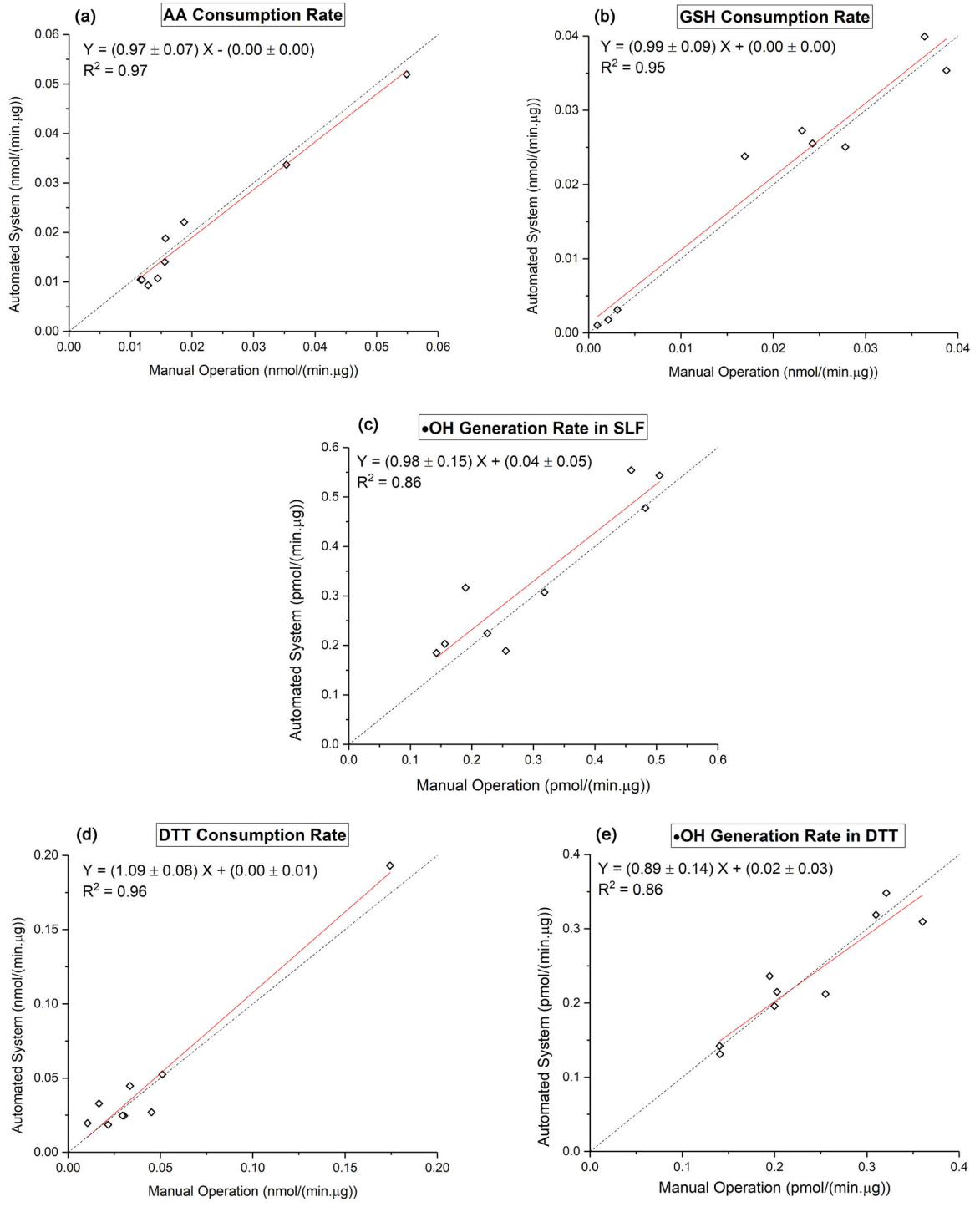


Figure 4. Comparison of manual operation (X axis) and automated system (Y axis) using ambient Hi-Vol filter samples (N = 9): (a) OP<sup>AA-SLF</sup>; (b) OP<sup>GSH-SLF</sup>; (c) OP<sup>OH-SLF</sup>; (d) OP<sup>OH-DTT</sup>. The identity line is plotted as the dotted line.

based studies (e.g., measuring oxidative stress in human lung adenocarcinoma cells) where the concentration of initial GSH is unknown and therefore it is important to measure both reduced (GSH) and oxidized (GSSG) glutathione to assess the cellular oxidative state. In the chemical assays, where we add a known amount of GSH, measurement of GSSG is not required and OP<sup>GSH</sup> can be simply determined by

measuring the oxidation rate of GSH. Nevertheless, Roušar et al. (2012) compared the GSH concentration from the conventional enzymatic recycling approach versus direct determination of GSH using OPA method, and reported an excellent agreement between two methods (slope from orthogonal fit = 0.98,  $R^2$  = 0.99, N = 45 biological samples). Note, the complexity of enzymatic recycling approach does not allow

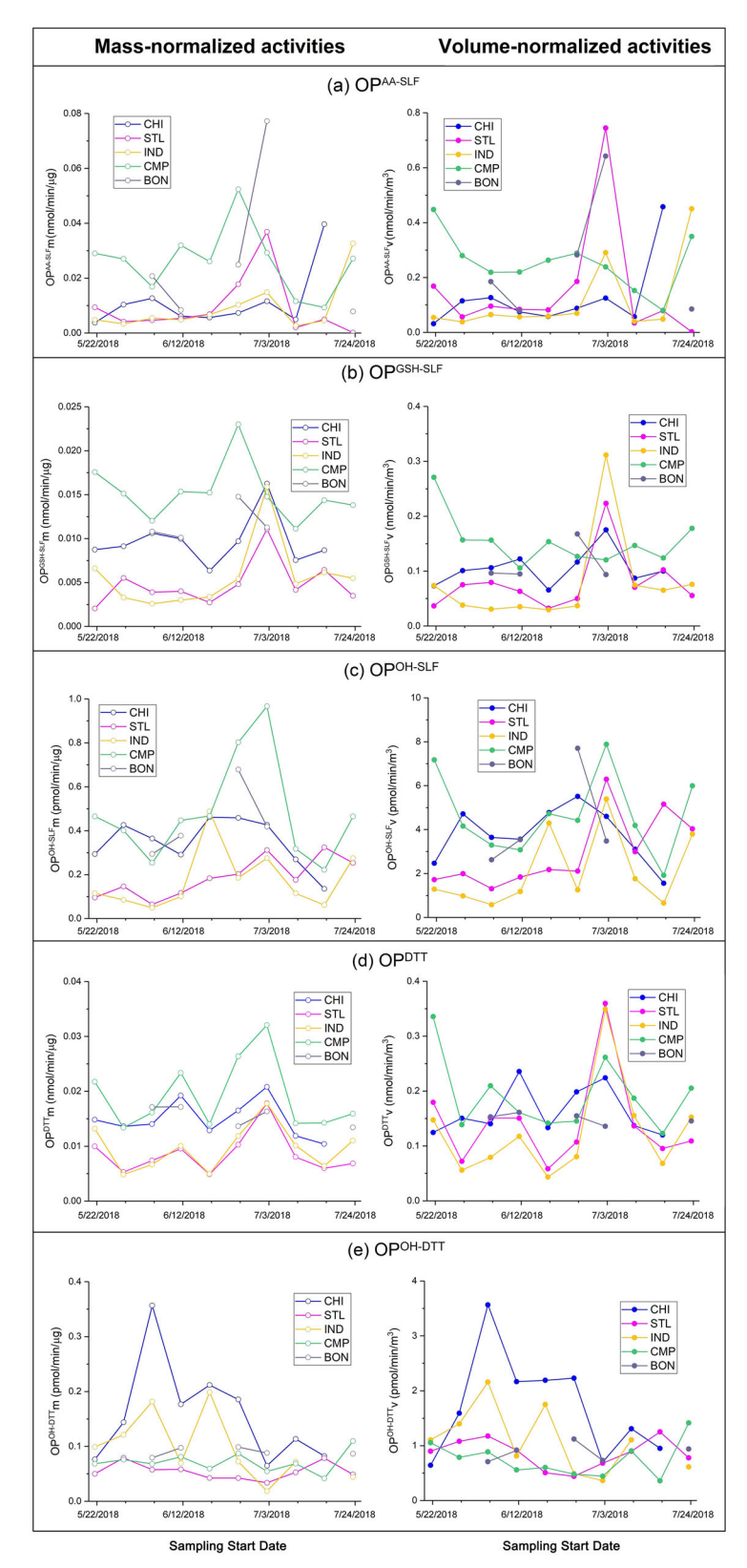


Figure 5. Mass and volume normalized OP of ambient  $PM_{2.5}$  using the Hi-Vol samples collected from five sites in the Midwest US (N = 44): (a)  $OP^{AA-SLF}$ ; (b)  $OP^{GSH-SLF}$ ; (c)  $OP^{OH-SLF}$ ; (d)  $OP^{OH-DTT}$ . Mass-normalized (OPm) and volume-normalized (OPv) of all samples are denoted by hollow and solid circles, respectively.

Table 4. Comparison of ambient PM2.5 OP obtained from SAMERA with those reported in the literatures.

Reference	PM size fraction (μm)	Levels	Location	Location type	Sample size
(a) OP <sup>AA</sup>					
Fang et al. (2016) <sup>a</sup>	<b>≤ 2.5</b>	$0.2 - 5.2  \text{nmol} \cdot \text{min}^{-1} \cdot \text{m}^{-3}$	Southeast US	Urban and rural	483
Mudway et al. (2005) <sup>b</sup>	<b>≤ 2.5</b>	$0.012 \pm 0.0001  \text{nmol·min}^{-1} \cdot \mu \text{g}^{-1}$	Eksaal, India	Biomass burning	3
Künzli et al. (2006) <sup>b</sup>	<b>≤ 2.5</b>	$0.0096 \pm 0.0025  \text{nmol·min}^{-1} \cdot \mu \text{g}^{-1}$	19 European cities	Urban	716
Szigeti et al. (2016) <sup>b,c</sup>	<b>≤ 2.5</b>	$0.0017 - 0.04  \text{nmol·min}^{-1} \cdot \mu \text{g}^{-1}$	8 European cities	Urban	22
Godri et al. (2011) <sup>b</sup>	1.0 - 1.9	$0.0058 \pm 0.0025  \text{nmol·min-1} \cdot \mu \text{g-1}$	London, United Kingdom	Urban	14
This study (OP <sup>AA-SLF</sup> )	<b>≤ 2.5</b>	$0.004 - 0.077  \text{nmol·min}^{-1} \cdot \mu \text{g}^{-1}$	Midwest US (5 sites)	Urban(4),rural(1)	54
		median: $0.012 \text{ nmol·min}^{-1} \cdot \mu g^{-1}$			
		$0.044 - 0.745  \text{nmol} \cdot \text{min}^{-1} \cdot \text{m}^{-3}$			
CSH		median: 0.160 nmol·min-1·m-3			
(b) OP <sup>GSH</sup>			· · · ·		_
Mudway et al. (2005) <sup>b</sup>	≤ 2.5	$0.0083 \pm 0.0002 \text{ nmol·min}^{-1} \cdot \mu g^{-1}$	Eksaal, India	Biomass burning	3
Künzli et al. (2006) <sup>b</sup>	≤ 2.5	$0.0041 \pm 0.0017 \text{ nmol·min}^{-1} \cdot \mu g^{-1}$	19 European cities	Urban	716
Szigeti et al. (2016) <sup>b,c</sup>	≤ 2.5	0 – 0.0275 nmol·min <sup>-1</sup> ·μg <sup>-1</sup>	8 European cities	Urban	22
Godri et al. (2011) <sup>b</sup>	1.0 – 1.9	$0.0042 \pm 0.0033$ nmol·min-1· $\mu$ g-1	London, United Kingdom	Urban	14
This study (OP <sup>GSH-SLF</sup> )	≤ 2.5	$0.001 - 0.040  \text{nmol·min}^{-1} \cdot \mu g^{-1}$	Midwest US (5 sites)	Urban(4),rural(1)	54
		median: $0.010 \text{ nmol} \cdot \text{min}^{-1} \cdot \mu g^{-1}$			
		$0.008 - 0.463  \text{nmol·min}^{-1} \cdot \text{m}^{-3}$			
(c) OP <sup>OH-SLF</sup>		median: 0.100 nmol⋅min <sup>-1</sup> ⋅m <sup>-3</sup>			
Vidrio et al. (2009) <sup>d</sup>	< 2.5	$0.253 \pm 0.135  \text{pmol·min}^{-1} \cdot \mu \text{g}^{-1}$	Davis, CA	Urban	~90
Ma et al. (2015) <sup>d</sup>	≤ 2.5 ≤ 2.5	$0.092 \pm 0.019  \text{pmol·min-1} \cdot \mu\text{g}$	Guangzhou, China	Urban	~90 72
This study	≤ 2.5 ≤ 2.5	$0.092 \pm 0.019  \text{pmol·min}^{-1} \cdot \mu \text{g}^{-1}$ $0.085 - 0.967  \text{pmol·min}^{-1} \cdot \mu \text{g}^{-1}$	Midwest US (5 sites)	Urban(4),rural(1)	72 54
This study	≥ 2.5	median: $0.307  \text{pmol·min}^{-1} \cdot \mu \text{g}^{-1}$	Midwest 03 (3 sites)	Orban(4),rurai(1)	34
		0.857 – 7.884 pmol·min <sup>-1</sup> ·m <sup>-3</sup>			
		median: 3.559 pmol·min-1·m-3			
(d) OP <sup>DTT</sup>		median. 5.555 pinor min 1 m 5			
Fang et al. (2016)	< 2.5	$0.15 - 0.43  \text{nmol·min}^{-1} \cdot \text{m}^{-3}$	Southeast US	Urban and rural	483
Xiong et al. (2017)	<u></u>	$0.1 - 0.18  \text{nmol} \cdot \text{min}^{-1} \cdot \text{m}^{-3}$	Urbana, IL	Urban	10
Verma et al. (2014)		$0.018 - 0.055  \text{nmol·min}^{-1} \cdot \mu \text{g}^{-1}$	Atlanta area, GA	Urban, rural	483
Cho et al. (2005)		$0.005 - 0.155  \text{nmol·min}^{-1} \cdot \mu \text{g}^{-1}$	Los Angeles basin, CA	Urban	11
Charrier et al. (2015)	<b>≤ 2.5</b>	$0.02 - 0.061  \text{nmol·min}^{-1} \cdot \mu \text{g}^{-1}$	San Joaquin, CA	Urban, rural	6
Hu et al. (2008)	0.25 - 2.5	0.014 − 0.024 nmol·min-1·µg-1	Los Angeles harbor, CA	Urban	84
This study	<b>≤ 2.5</b>	$0.004 - 0.193  \text{nmol·min}^{-1} \cdot \mu \text{g}^{-1}$	Midwest US (5 sites)	Urban(4),rural(1)	54
·		median: $0.014  \text{nmol} \cdot \text{min}^{-1} \cdot \mu \text{g}^{-1}$			
		$0.041 - 1.282  \text{nmol·min}^{-1} \cdot \text{m}^{-3}$			
		median: 0.146 nmol·min-1·m-3			
(e) OP <sup>OH-DTT</sup>					
Xiong et al. (2017)	≤ 2.5	$0.2 - 0.6 \mathrm{pmol \cdot min^{-1} \cdot m^{-3}}$	Urbana, IL	Urban	10
Yu et al. (2018)	≤ 2.5	0.2 – 1.1 pmol·min <sup>-1</sup> ·m <sup>-3</sup>	Urbana, IL	Urban	10
This study	≤ 2.5	$0.034 - 0.357  \text{pmol·min}^{-1} \cdot \mu \text{g}^{-1}$	Midwest US (5 sites)	Urban(4),rural(1)	54
		median: $0.082  \text{pmol·min}^{-1} \cdot \mu \text{g}^{-1}$			
		0.360 – 4.152 pmol·min <sup>-1</sup> ·m <sup>-3</sup>			
		median: 1.054 pmol·min <sup>-1</sup> ·m <sup>-3</sup>			

<sup>a</sup>The study assessed OPAA of ambient PM samples in an AA-only model (no other antioxidants involved).

measuring the kinetic properties of GSH depletion as yielded by SAMERA, which could be important to understand the reaction mechanism and the role of different chemical components in this OP endpoint.

In contrast to OP<sup>AA</sup> and OP<sup>GSH</sup>, fewer studies have used OP<sup>OH-SLF</sup> endpoint. Similar to OP<sup>GSH-SLF</sup>, Table 4c shows a wider range of OP<sup>OH-SLF</sup> in our analysis compared to two studies (Ma et al. 2015; Vidrio et al. 2009) using the same SLF protocol. Note, due to the lack of kinetic profile, •OH generation rates from these two studies were calculated assuming a linear pattern of •OH production within 24 h, which could lead to erroneous estimates. Therefore, caution needs

to be exercised in comparing these results. Moreover, the samples used in those two studies were collected from a single site (i.e., Davis, CA for Vidrio et al. [2009] and Guangzhou, China for Ma et al. [2015]), in contrast to our samples, which were collected from five different sites, probably resulting into a wider range of OP activities in our study.

As the most commonly used endpoint,  $OP^{DTT}$  has the largest database in existing literature. Both mass-normalized and volume-normalized DTT activities measured in this study are in good agreement with those from many previous studies listed in Table 4d (i.e., within the typical range:  $0.005-0.2 \text{ nmol min}^{-1} \cdot \mu g^{-1}$  for

bThe composition of lung lining fluid (200 μM AA, 200 μM GSH, and 200 μM UA) was different in these studies than the SLF used in our study. Moreover, total consumption of AA and GSH in 4h was reported, and we have estimated the rates assuming linear pattern of AA and GSH consumption with time.

<sup>&</sup>lt;sup>c</sup>The author compared the OP activities between indoor air PM and outdoor air PM. Only the results of outdoor air PM were included in this table.

<sup>&</sup>lt;sup>d</sup>The SLF used in these studies had the same composition as ours (200 μM AA, 100 μM GSH, 100 μM UA, and 300 μM CA). However, total •OH generated in 24 h was reported, and we have estimated the rates assuming linear pattern of •OH generation with time.



 $\text{OP}^{\text{DTT}}\text{m}$  and 0.1–0.5  $\text{nmol}\cdot\text{min}^{-1}\cdot\text{m}^{-3}$  for  $\text{OP}^{\text{DTT}}\text{v}).$  In contrast, OP<sup>OH-DTT</sup> is a newer endpoint which was first introduced in our previous study (Xiong et al. 2017). The activity of OPOH-DTT measured in this study is significantly higher than our previous studies [i.e., Xiong et al. [2017] and Yu et al. [2018] [Table 4e]) reporting this endpoint. This is again attributed to a diversity of the sites we have in the current study in contrast to only two sites, which were both in Champaign (IL) in those studies. Interestingly, the range of OPOH-DTT v at CMP in this study  $(0.4-1.4 \,\mathrm{pmol \cdot min^{-1} \cdot m^{-3}};$  Figure 5e) is close to that reported in our previous study Yu et al. (2018)  $(0.2-1.1 \text{ pmol} \cdot \text{min}^{-1} \cdot \text{m}^{-3})$ , indicating the consistency of our automated protocol. Further investigation of PM chemical composition (currently underway), will help in revealing the complex patterns of these OP endpoints among different sites.

#### 4. Conclusions

SAMERA is designed for an automated analysis of five OP endpoints – OP<sup>AA-SLF</sup>, OP<sup>GSH-SLF</sup>, OP<sup>OH-SLF</sup>, OP<sup>DTT</sup> and OPOH-DTT on ambient PM aqueous extracts. Both spectrophotometric- and spectrofluorometric-based approaches were adopted to obtain a simultaneous measurement of multiple endpoints. The system analyzes all five OP endpoints for a given sample within 3 h. The precision tests on SAMERA demonstrated a high reproducibility for both positive controls and ambient PM<sub>2.5</sub> samples. The measurements obtained from SAMERA are also highly accurate as they were validated against the results from manual operation using the same experimental protocol. We recommend a liquid concentration of ambient PM<sub>2.5</sub> extracts in the reaction mixture as 50 µg/mL for the SLF-based assays, and 30 μg/mL for DTT-based assays.

Overall, SAMERA provides the first rapid and highthroughput analysis protocol for multiple endpoints of OP. It substantially reduces the time and labor required to conduct various OP assays on the ambient PM samples, which will facilitate integrating the OP dataset into epidemiological models in future studies. Furthermore, SAMERA can yield the kinetic properties for antioxidant (e.g., GSH) consumption and ROS generation (e.g., •OH generation in SLF), which have not been typically obtained in previous studies due to labor-intensive protocols of these endpoints. The study also explored the feasibility of employing SAMERA for analyzing a large set of ambient PM<sub>2.5</sub> samples currently being collected from the Midwest US. Preliminary results show that the range of OP activities obtained from SAMERA is broader than those reported in previous studies, which

is probably due to the diversity in chemical composition of the ambient samples collected from five different sampling sites in our study. The activities for most OP endpoints were significantly elevated in the week of July 4 at all the sites, indicating a substantial impact of fireworks emissions from Independence Day celebration on ambient PM<sub>2.5</sub> OP. Further analysis of OP on the remaining samples along with a detailed chemical speciation, which is currently underway, will yield insights on the chemical components and their emission sources contributing to different mechanisms of ROS generation induced by ambient  $PM_{2.5}$  in the Midwest US.

#### **Funding**

This material is based upon work supported by the Science Foundation under Grant CBET-1847237.

#### **ORCID**

Haoran Yu http://orcid.org/0000-0003-4464-0387

#### References

Abrams, J. Y., R. J. Weber, M. Klein, S. E. Samat, H. H. Chang, M. J. Strickland, V. Verma, T. Fang, J. T. Bates, J. A. Mulholland, A. G. Russell, and P. E. Tolbert. 2017. Associations between ambient fine particulate oxidative potential and cardiorespiratory emergency department visits. Environ. Health Perspect. 125 (10):107008. doi:10. 1289/EHP1545.

Alfadda, A. A., and R. M. Sallam. 2012. Reactive oxygen species in health and disease. BioMed Res. Int. 2012:1-14. doi:10.1155/2012/936486.

Antiñolo, M., M. D. Willis, S. Zhou, and J. P. Abbatt. 2015. Connecting the oxidation of soot to its redox cycling abilities. Nature Commun. 6 (1):66812. doi:10.1038/ ncomms7812.

Araujo, J. A., and A. E. Nel. 2009. Particulate matter and atherosclerosis: role of particle size, composition and oxidative stress. Particle Fibre Toxicol. 6 (1):24. doi:10.1186/ 1743-8977-6-24.

Ayres, J. G., P. Borm, F. R. Cassee, V. Castranova, K. Donaldson, A. Ghio, R. M. Harrison, R. Hider, F. Kelly, I. M. Kooter, et al. 2008. Evaluating the toxicity of airborne particulate matter and nanoparticles by measuring oxidative stress potential—a workshop report and consensus statement. Inhal. Toxicol. 20 (1):75-99. doi:10. 1080/08958370701665517.

Böhmer, A., J. Jordan, and D. Tsikas. 2011. High-performance liquid chromatography ultraviolet assay for human erythrocytic catalase activity by measuring glutathione as o-phthalaldehyde derivative. Anal. Biochem. 410 (2): 296-303. doi:10.1016/j.ab.2010.11.026.

Baker, M. A., G. J. Cerniglia, and A. Zaman. 1990. Microtiter plate assay for the measurement of glutathione

- and glutathione disulfide in large numbers of biological samples. Anal. Biochem. 190 (2):360-365. doi:10.1016/ 0003-2697(90)90208-Q.
- Bates, J. T., R. J. Weber, J. Abrams, V. Verma, T. Fang, M. Klein, M. J. Strickland, S. E. Sarnat, H. H. Chang, and J. A. Mulholland. 2015. Reactive oxygen species generation linked to sources of atmospheric particulate matter and cardiorespiratory effects. Environmental Sci. Technol. 49 (22):13605-13612. doi:10.1021/acs.est.5b02967.
- Becker, S., L. A. Dailey, J. M. Soukup, S. C. Grambow, R. B. Devlin, and Y.-C. T. Huang. 2005. Seasonal variations in air pollution particle-induced inflammatory mediator release and oxidative stress. Environ. Health Perspect. 113 (8):1032-1038. doi:10.1289/ehp.7996.
- Birben, E., U. M. Sahiner, C. Sackesen, S. Erzurum, and O. Kalayci. 2012. Oxidative stress and antioxidant defense. World Allergy Org. J. 5 (1):9. doi:10.1097/WOX. 0b013e3182439613.
- Bonomini, F., S. Tengattini, A. Fabiano, R. Bianchi, and R. Rezzani. 2008. Atherosclerosis and oxidative stress. Histol. Histopathol. 23 (3):381-390. doi:10.14670/HH-23.
- Charrier, J., and C. Anastasio. 2012. On dithiothreitol (DTT) as a measure of oxidative potential for ambient particles: evidence for the importance of soluble transition metals. Atmos. Chem. Phys. 12 (19):9321. doi:10. 5194/acp-12-9321-2012.
- Charrier, J. G., and C. Anastasio. 2015. Rates of hydroxyl radical production from transition metals and quinones in a surrogate lung fluid. Environ. Sci. Technol. 49 (15): 9317-9325. doi:10.1021/acs.est.5b01606.
- Charrier, J. G., A. S. McFall, N. K. Richards-Henderson, and C. Anastasio. 2014. Hydrogen peroxide formation in a surrogate lung fluid by transition metals and quinones present in particulate matter. Environ. Sci. Technol. 48 (12):7010-7017. doi:10.1021/es501011w.
- Charrier, J., N. Richards-Henderson, K. Bein, A. McFall, A. Wexler, and C. Anastasio. 2015. Oxidant production from source-oriented particulate matter-Part 1: oxidative potential using the dithiothreitol (DTT) assay. Atmos. Chem. Phys. (15):2327-2340. doi:10.5194/acp-15-2327-2015.
- Charrier, J. G., A. S. McFall, K. K. Vu, J. Baroi, C. Olea, A. Hasson, and C. Anastasio. 2016. A bias in the "mass-normalized" DTT response-an effect of non-linear concentration-response curves for copper and manganese. Atmos. Environ. 144:325-334. doi:10.1016/j.atmosenv. 2016.08.071.
- Cho, A. K., C. Sioutas, A. H. Miguel, Y. Kumagai, D. A. Schmitz, M. Singh, A. Eiguren-Fernandez, and J. R. Froines. 2005. Redox activity of airborne particulate matter at different sites in the Los Angeles Basin. Environ. Res. 99 (1):40-47. doi:10.1016/j.envres.2005.01.003.
- Chuang, K.-J., C.-C. Chan, T.-C. Su, C.-T. Lee, and C.-S. Tang. 2007. The effect of urban air pollution on inflammation, oxidative stress, coagulation, and autonomic dysfunction in young adults. Am. J. Resp. Crit. Care Med. 176 (4):370-376. doi:10.1164/rccm.200611-1627OC.
- Cohen, A. J., M. Brauer, R. Burnett, H. R. Anderson, J. Frostad, K. Estep, K. Balakrishnan, B. Brunekreef, L. Dandona, R. Dandona, et al. 2017. Estimates and 25-year trends of the global burden of disease attributable to

- ambient air pollution: an analysis of data from the global burden of diseases study 2015. Lancet 389 (10082): 1907-1918. doi:10.1016/S0140-6736(17)30505-6.
- Crobeddu, B., L. Aragao-Santiago, L.-C. Bui, S. Boland, and A. B. Squiban. 2017. Oxidative potential of particulate matter 2.5 as predictive indicator of cellular stress. Environ. Pollut. 230:125-133. doi:10.1016/j.envpol.2017. 06.051.
- D'Autréaux, B., and M. B. Toledano. 2007. ROS as signalling molecules: mechanisms that generate specificity in ROS homeostasis. Nat. Rev. Mol. Cell Biol. 8 (10):813. doi:10.1038/nrm2256.
- Delfino, R. J., N. Staimer, T. Tjoa, D. L. Gillen, J. J. Schauer, and M. M. Shafer. 2013. Airway inflammation and oxidative potential of air pollutant particles in a pediatric asthma panel. J. Exposure Sci. Environ. Epidemiol. 23 (5):466-473. doi:10.1038/jes.2013.25.
- Fang, T., V. Verma, J. T. Bates, J. Abrams, M. Klein, M. J. Strickland, S. E. Sarnat, H. H. Chang, J. A. Mulholland, P. E. Tolbert, et al. 2016. Oxidative potential of ambient water-soluble PM 2.5 in the southeastern United States: contrasts in sources and health associations between ascorbic acid (AA) and dithiothreitol (DTT) assays. Atmos. Chem. Phys. 16 (6):3865-3879. doi:10.5194/acp-16-3865-2016.
- Fang, T., V. Verma, H. Guo, L. King, E. Edgerton, and R. Weber. 2014. A semi-automated system for quantifying the oxidative potential of ambient particles in aqueous extracts using the dithiothreitol (DTT) assay: results from the Southeastern Center for Air Pollution and Epidemiology (SCAPE). Atmos. Meas. Tech. Discussions 7 (7):7245. doi:10.5194/amt-8-471-2015.
- Feng, S., D. Gao, F. Liao, F. Zhou, and X. Wang. 2016. The health effects of ambient PM2.5 and potential mechanisms. Ecotoxicol. Environ. Safety 128::67-74. doi:10. 1016/j.ecoenv.2016.01.030.
- Godri, K. J., R. M. Harrison, T. Evans, T. Baker, C. Dunster, I. S. Mudway, and F. J. Kelly. 2011. Increased oxidative burden associated with traffic component of ambient particulate matter at roadside and urban background schools sites in London. PLoS One 6 (7):e21961. doi:10.1371/journal.pone.0021961.
- Held, K. D., F. C. Sylvester, K. L. Hopcia, and J. E. Biaglow. 1996. Role of Fenton chemistry in thiol-induced toxicity and apoptosis. Radiation Res. 145 (5):542-553. doi:10. 2307/3579272.
- Hu, S., A. Polidori, M. Arhami, M. Shafer, J. Schauer, A. Cho, and C. Sioutas. 2008. Redox activity and chemical speciation of size fractioned PM in the communities of the Los Angeles-Long Beach harbor. Atmos. Chem. Phys. 8 (21):6439-6451. doi:10.5194/acp-8-6439-2008.
- Hulskotte, J., H. Denier van der Gon, A. Visschedijk, and M. Schaap. 2007. Brake wear from vehicles as an important source of diffuse copper pollution. Water Sci. Technol. 56 (1):223-231. doi:10.2166/wst.2007.456.
- Janssen, N. A., M. Strak, A. Yang, B. Hellack, F. J. Kelly, T. A. Kuhlbusch, R. M. Harrison, B. Brunekreef, F. R. Cassee, and M. Steenhof. 2015. Associations between three specific a-cellular measures of the oxidative potential of particulate matter and markers of acute airway inflammation in healthy volunteers.



- Occupational Environ. Med. 72 (1):49-56. doi:10.1136/ oemed-2014-102303.
- Janssen, N. A. H., A. Yang, M. Strak, M. Steenhof, B. Hellack, M. E. Gerlofs-Nijland, T. Kuhlbusch, F. Kelly, R. Harrison, B. Brunekreef, et al. 2014. Oxidative potential of particulate matter collected at sites with different source characteristics. Sci. Total Environ. 472:572-581. doi:10.1016/j.scitotenv.2013.11.099.
- Künzli, N., I. S. Mudway, T. Götschi, T. Shi, F. J. Kelly, S. Cook, P. Burney, B. Forsberg, J. W. Gauderman, M. E. Hazenkamp, et al. 2006. Comparison of oxidative properties, light absorbance, and total and elemental mass concentration of ambient PM2. 5 collected at 20 European sites. Environ. Health Perspect. 114 (5):684-690. doi:10. 1289/ehp.8584.
- Kampa, M., and E. Castanas. 2008. Human health effects of air pollution. Environ. Pollut. 151 (2):362-367. doi:10. 1016/j.envpol.2007.06.012.
- Knaapen, A. M., P. J. Borm, C. Albrecht, and R. P. Schins. 2004. Inhaled particles and lung cancer. Part A: Mechanisms. Int. J. Cancer 109 (6):799-809. doi:10.1002/
- Kodavanti, U. P., M. C. Schladweiler, A. D. Ledbetter, W. P. Watkinson, M. J. Campen, D. W. Winsett, J. R. Richards, K. M. Crissman, G. E. Hatch, and D. L. Costa. 2000. The spontaneously hypertensive rat as a model of human cardiovascular disease: evidence of exacerbated cardiopulmonary injury and oxidative stress from inhaled emission particulate matter. Toxicol. Appl. Pharmacol. 164 (3): 250-263. doi:10.1006/taap.2000.8899.
- Li, N., C. Sioutas, A. Cho, D. Schmitz, C. Misra, J. Sempf, M. Wang, T. Oberley, J. Froines, and A. Nel. 2003. Ultrafine particulate pollutants induce oxidative stress and mitochondrial damage. Environ. Health Perspect. 111 (4):455. doi:10.1289/ehp.6000.
- Li, N., T. Xia, and A. E. Nel. 2008. The role of oxidative stress in ambient particulate matter-induced lung diseases and its implications in the toxicity of engineered nanoparticles. Free Radical Biol. Med. 44 (9):1689-1699. doi: 10.1016/j.freeradbiomed.2008.01.028.
- Longhin, E., J. A. Holme, K. B. Gutzkow, V. M. Arlt, J. E. Kucab, M. Camatini, and M. Gualtieri. 2013. Cell cycle alterations induced by urban PM2. 5 in bronchial epithelial cells: characterization of the process and possible mechanisms involved. Particle Fibre Toxicol. 10 (1):63. doi:10.1186/1743-8977-10-63.
- Ma, S., K. Ren, X. Liu, L. Chen, M. Li, X. Li, J. Yang, B. Huang, M. Zheng, and Z. Xu. 2015. Production of hydroxyl radicals from Fe-containing fine particles in Guangzhou, China. Atmos. Environ. 123:72-78. doi:10. 1016/j.atmosenv.2015.10.057.
- Maikawa, C. L., S. Weichenthal, A. J. Wheeler, N. A. Dobbin, A. Smargiassi, G. Evans, L. Liu, M. S. Goldberg, and K. J. G. Pollitt. 2016. Particulate oxidative burden as a predictor of exhaled nitric oxide in children with asthma. Environ. Health Perspect. 124 (10):1616. doi:10. 1289/EHP175.
- Mudway, I. S., S. T. Duggan, C. Venkataraman, G. Habib, F. J. Kelly, and J. Grigg. 2005. Combustion of dried animal dung as biofuel results in the generation of highly redox active fine particulates. Particle Fibre Toxicol. 2 (1): 6. doi:10.1186/1743-8977-2-6.

- Mudway, I. S., N. Stenfors, A. Blomberg, R. Helleday, C. Dunster, S. Marklund, A. J. Frew, T. Sandström, and F. J. Kelly. 2001. Differences in basal airway antioxidant concentrations are not predictive of individual responsiveness to ozone: a comparison of healthy and mild asthmatic subjects. Free Radical Biol. Med. 31 (8):962-974. doi:10. 1016/S0891-5849(01)00671-2.
- Oh, S. M., H. R. Kim, Y. J. Park, S. Y. Lee, and K. H. Chung. 2011. Organic extracts of urban air pollution particulate matter (PM2. 5)-induced genotoxicity and oxidative stress in human lung bronchial epithelial cells (BEAS-2B cells). Mutation Res./Genetic Toxicol. Environ. Mutagenesis 723 (2):142-151. doi:10.1016/j.mrgentox. 2011.04.003.
- Pervez, S., R. K. Chakrabarty, S. Dewangan, J. G. Watson, J. C. Chow, and J. L. Matawle. 2016. Chemical speciation of aerosols and air quality degradation during the festival of lights (Diwali). Atmos.c Pollution Res. 7 (1):92-99. doi: 10.1016/j.apr.2015.09.002.
- Pham-Huy, L. A. H., He, and C. Pham-Huy. 2008. Free radicals, antioxidants in disease and health. Int. J. Biomed.
- Pietrogrande, M. C., I. Bertoli, F. Manarini, and M. Russo. 2019. Ascorbate assay as a measure of oxidative potential for ambient particles: Evidence for the importance of cell-free surrogate lung fluid composition. Atmos. Environ. 211 (2019):103-112. doi:10.1016/j.atmosenv. 2019.05.012.
- Puthussery, J. V. C., Zhang, and V. Verma. 2018. Development and field testing of an online instrument for measuring the real-time oxidative potential of ambient particulate matter based on dithiothreitol assay. Atmos. Meas. Tech. 11 (10):5767-5780. doi:10.5194/amt-11-5767-2018.
- Rahman, T., I. Hosen, M. T. Islam, and H. U. Shekhar. 2012. Oxidative stress and human health. Adv. Biosci. Biotechnol. 3 (7):997. doi:10.4236/abb.2012.327123.
- Roušar, T., O. Kučera, H. Lotková, and Z. Červinková. 2012. Assessment of reduced glutathione: comparison of an optimized fluorometric assay with enzymatic recycling method. Anal. Biochem. 423 (2):236-240. doi:10.1016/j. ab.2012.01.030.
- Saffari, A., N. Daher, M. M. Shafer, J. J. Schauer, and C. Sioutas. 2014. Seasonal and spatial variation in dithiothreitol (DTT) activity of quasi-ultrafine particles in the Los Angeles Basin and its association with chemical species. J. Environ. Sci. Health, Part A 49 (4):441-451. doi: 10.1080/10934529.2014.854677.
- Sarnat, S. E., H. H. Chang, and R. J. Weber. 2016. Ambient PM2. 5 and health: does PM2. 5 oxidative potential play a role? Am. J. Respir. Crit. Care Med. (194):530-531. doi: 10.1164/rccm.201603-0589ED.
- Sauvain, J.-J., S. Deslarzes, F. Storti, and M. Riediker. 2015. Oxidative potential of particles in different occupational environments: a pilot study. Ann. Occupational Hygiene 59 (7):882-894. doi:10.1093/annhyg/mev024.
- Shen, H. A., Barakat, and C. Anastasio. 2011. Generation of hydrogen peroxide from San Joaquin Valley particles in a cell-free solution. Atmos. Chem. Phys. 11 (2):753-765. doi:10.5194/acp-11-753-2011.
- Son, Y., V. Mishin, W. Welsh, S.-E. Lu, J. D. Laskin, H. Kipen, and Q. Meng. 2015. A novel high-throughput

- approach to measure hydroxyl radicals induced by airborne particulate matter. Int. J. Environ. Res. Public Health 12 (11):13678–13695. doi:10.3390/ ijerph121113678.
- Sun, Q., A. Wang, X. Jin, A. Natanzon, D. Duquaine, R. D. Brook, J.-G. S. Aguinaldo, Z. A. Fayad, V. Fuster, and M. Lippmann. 2005. Long-term air pollution exposure and acceleration of atherosclerosis and vascular inflammation in an animal model. JAMA 294 (23):3003-3010. doi:10. 1001/jama.294.23.3003.
- Szigeti, T., C. Dunster, A. Cattaneo, D. Cavallo, A. Spinazzè, D. E. Saraga, I. A. Sakellaris, Y. de Kluizenaar, E. J. Cornelissen, and O. Hänninen. 2016. Oxidative potential and chemical composition of PM2.5 in office buildings across Europe-the OFFICAIR study. Environ. *Int.* 92:324–333. doi:10.1016/j.envint.2016.04.015.
- Torres-Ramos, Y. D., A. Montoya-Estrada, A. M. Guzman-Grenfell, J. Mancilla-Ramirez, B. Cardenas-Gonzalez, S. Blanco-Jimenez, J. D. Sepulveda-Sanchez, A. Ramirez-Venegas, and J. J. Hicks. 2011. Urban PM2.5 induces ROS generation and RBC damage in COPD patients. Frontiers Biosci. (Elite Edition) 3 E (3):808-817. doi:10. 2741/e288.
- Verma, V., T. Fang, H. Guo, L. King, J. Bates, R. Peltier, E. Edgerton, A. Russell, and R. Weber. 2014. Reactive oxygen species associated with water-soluble PM 2.5 in the southeastern United States: spatiotemporal trends and source apportionment. Atmos. Chem. Phys. (14): 12915-12930. doi:10.5194/acp-14-12915-2014.
- Verma, V., T. Fang, L. Xu, R. E. Peltier, A. G. Russell, N. L. Ng, and R. J. Weber. 2015a. Organic aerosols associated with the generation of reactive oxygen species (ROS) by water-soluble PM2. 5. Environ. Sci. Technol. 49 (7): 4646-4656. doi:10.1021/es505577w.
- Verma, V., Z. Ning, A. K. Cho, J. J. Schauer, M. M. Shafer, and C. Sioutas. 2009. Redox activity of urban quasi-ultrafine particles from primary and secondary sources. Atmos. Environ. 43 (40):6360-6368. doi:10.1016/j.atmosenv.2009.09.019.
- Verma, V., R. Rico-Martinez, N. Kotra, L. King, J. Liu, T. W. Snell, and R. J. Weber. 2012. Contribution of water-soluble and insoluble components and their hydrophobic/hydrophilic subfractions to the reactive oxygen species-generating potential of fine ambient aerosols. Environ. Sci. Technol. 46 (20):11384-11392. doi:10.1021/ es302484r.
- Verma, V., Y. Wang, R. El-Afifi, T. Fang, J. Rowland, A. G. Russell, and R. J. Weber. 2015b. Fractionating ambient humic-like substances (HULIS) for their reactive oxygen species activity-assessing the importance of quinones and atmospheric aging. Atmos. Environ. 120:351-359. doi:10. 1016/j.atmosenv.2015.09.010.
- Vidrio, E., H. Jung, and C. Anastasio. 2008. Generation of hydroxyl radicals from dissolved transition metals in surrogate lung fluid solutions. Atmos. Environ. 42 (18): 4369-4379. doi:10.1016/j.atmosenv.2008.01.004.

- Vidrio, E., C. H. Phuah, A. M. Dillner, and C. Anastasio. 2009. Generation of hydroxyl radicals from ambient fine particles in a surrogate lung fluid solution. Environ. Sci. Technol. 43 (3):922-927. doi:10.1021/ es801653u.
- Visentin, M., A. Pagnoni, E. Sarti, and M. C. Pietrogrande. 2016. Urban PM2. 5 oxidative potential: Importance of chemical species and comparison of two spectrophotometric cell-free assays. Environ. Pollut. 219:72-79. doi:10. 1016/j.envpol.2016.09.047.
- Wang, Y., M. J. Plewa, U. K. Mukherjee, and V. Verma. 2018. Assessing the cytotoxicity of ambient particulate matter (PM) using Chinese hamster ovary (CHO) cells and its relationship with the PM chemical composition and oxidative potential. Atmos. Environ. 179:132-141. doi:10.1016/j.atmosenv.2018.02.025.
- Weichenthal, S., E. Lavigne, G. Evans, K. Pollitt, and R. T. Burnett. 2016. Ambient PM2.5 and risk of emergency room visits for myocardial infarction: impact of regional PM2.5 oxidative potential: a case-crossover study. Environ. Health 15 (1):46. doi:10.1186/s12940-016-0129-9.
- West, J. J., A. Cohen, F. Dentener, B. Brunekreef, T. Zhu, B. Armstrong, M. L. Bell, M. Brauer, G. Carmichael, and D. L. Costa. 2016. What we breathe impacts our health: improving understanding of the link between air pollution and health. Environ. Sci. Technol. 50 (10):4895-4904. doi:10.1021/acs.est.5b03827.
- Xiong, Q., H. Yu, R. Wang, J. Wei, and V. Verma. 2017. Rethinking the dithiothreitol (DTT) based PM oxidative potential: Measuring DTT consumption versus ROS generation. Environ. Sci. Technol. 51 (11):6507-6514. doi:10. 1021/acs.est.7b01272.
- Yan, Z., J. Wang, J. Li, N. Jiang, R. Zhang, W. Yang, W. Yao, and W. Wu. 2016. Oxidative stress and endocytosis are involved in upregulation of interleukin-8 expression in airway cells exposed to PM 2.5. Environ. Toxicol. 31 (12):1869-1878. doi:10.1002/tox.22188.
- Yang, A., N. A. Janssen, B. Brunekreef, F. R. Cassee, G. Hoek, and U. Gehring. 2016. Children's respiratory health and oxidative potential of PM2.5: the PIAMA birth cohort study. Occupational Environ. Med. 73 (3): 154-160. doi:10.1136/oemed-2015-103175.
- Yu, H., J. Wei, Y. Cheng, K. Subedi, and V. Verma. 2018. Synergistic and antagonistic interactions among the particulate matter components in generating reactive oxygen species based on the dithiothreitol assay. Environ. Sci. Technol. 52 (4):2261-2270. doi:10.1021/acs.est.7b04261.
- Zhang, X., N. Staimer, D. L. Gillen, T. Tjoa, J. J. Schauer, M. M. Shafer, S. Hasheminassab, P. Pakbin, N. D. Vaziri, C. Sioutas, and R. J. Delfino. 2016. Associations of oxidative stress and inflammatory biomarkers with chemically-characterized air pollutant exposures in an elderly cohort. Environ. Res. 150:306-319. doi:10.1016/j. envres.2016.06.019.